ELSEVIER

Journal of Alloys and Compounds 330–332 (2002) 219–224

Journal of ALLOYS AND COMPOUNDS

www.elsevier.com/locate/jallcom

# H-induced phase separation in Pd–Pt alloys as studied by high resolution electron microscopy

R. Lüke[a], G. Schmitz[a], T.B. Flanagan[b], R. Kirchheim[a,*]

[a]*Institut für Materialphysik, Der Georg-August-Universität Göttingen, Hospitalstr. 3–7, D-37073 Göttingen, Germany*
[b]*Department of Chemistry, University of Vermont, Burlington, VT 05405, USA*

**Abstract**

$Pd_{80}Pt_{20}$ and $Pd_{85}Pt_{15}$ alloys were exposed at 673 K to a hydrogen pressure of 100 MPa for 4 h, which is called hydrogen heat treatment (HHT). After HHT the pressure composition isotherms at 273 K change remarkably and H-diffusion is enhanced. The change can be interpreted by a decomposition into a continuous Pd-rich and an embedded Pt-rich alloy. Direct evidence for this hypothesis is provided for the first time from high resolution electron microscopy. It will be shown that coherent platelets are formed after HHT which are two atomic layers thick and have an average diameter of ~10 nm. Simulating the contrast observed in the electron microscope shows that the plates are Pt-rich. 

*Keywords:* Hydrogen in metals; Hydrogen diffusion; Decomposition; Electron microscopy

## 1. Introduction

From interpreting pressure composition isotherms it has been concluded by Flanagan et al. [1,2] that Pd–Pt alloys decompose into Pd-rich and Pt-rich phases after hydrogen heat treatment (HHT), i.e. exposure of the alloy to high temperatures and high hydrogen pressures. Some additional evidence was provided [2] by transmission electron microscopy (TEM) and small angle neutron scattering (SANS). Direct imaging of the morphology of the decomposed alloy has not been achieved so far and it is the subject of the present paper.

The detailed analysis in Ref. [2] demonstrates that Pd–Pt alloys with Pt-contents between 0 and 30 at.% decompose at 673 K into two phases if hydrogen is added as a third component. Besides its role as a third component providing the driving force for the decomposition, hydrogen also enhances the lattice mobility of the substitutional components Pd and Pt and, therefore, the kinetics of the decomposition become fast enough to take place at the rather low reduced temperatures of $T/T_m \approx 0.35$ (where $T_m$ is the melting temperature of the metal).

In the present study we will mainly discuss the alloy $Pd_{80}Pt_{20}$ as prepared and after HHT (at 673 K, 1000 MPa, 3 h); if not stated otherwise, most of the results are similar for the $Pd_{85}Pt_{15}$ alloy which was also investigated. In the first case the plateau pressure after HHT corresponded to a composition of $Pd_{93}Pt_{07}$, i.e. in the framework of the interpretation provided in Ref. [2], this corresponds to the composition of the Pd-rich phase. From the length of the plateau a volume fraction of 0.6 was evaluated and, therefore, the Pt-rich phase should be present with a volume fraction of 0.4 and a composition of $Pd_{60}Pt_{40}$. The decomposition after HHT is accompanied by the formation of dislocations and additional strain, probably stemming from the misfit of coherent precipitates. High resolution TEM (HREM) and analytical TEM also revealed considerable strain and Pt-rich regions, however, no direct images of the two phases were obtained. By using SANS a particle/particle correlation peak was measured for a $Pd_{75}Pt_{25}$ alloy after HHT yielding an average distance of the particles of 3.7 nm.

In this work we used HREM to analyze the morphology of the phases formed in $Pd_{80}Pt_{20}$ and $Pd_{85}Pt_{15}$ as prepared and after HHT. In addition H-diffusion coefficients were measured in these samples by the electrochemical technique previously employed by Kirchheim [3].

## 2. Experimental procedure and results

Samples were prepared as thin foils of 60–100-μm

*Corresponding author. Tel.: +49-551-395-001; fax: +49-551-395-012.

*E-mail address:* rkirch@umpa03.gwdg.de (R. Kirchheim).

0925-8388/02/$ – see front matter 
PII: S0925-8388(01)01590-0

thickness as described in Ref. [2]. Discs with a diameter of 3 mm were punched out of these foils and thinned by ion milling. The ions had an energy of 6 kV with an angle of incidence of 20° to the sample surface. After electron transparency had been reached the parameters were changed to 3.5 kV and 15°. In order to remove near surface regions damaged by the high energy ions, the samples were electropolished in perchloric and acetic acid (1:3) for 4 min at 275 K. HREM was performed with a CEM 200 FEG Philips electron microscope (point resolution: 0.18 nm) in a symmetric five beam configuration using the four (200) diffracted beams.

In Fig. 1 the microstructures of the as received and the HHT sample of $Pd_{80}Pt_{20}$ are shown at a relatively low magnification. Whereas the untreated sample contained a few dislocations only, the HHT sample had a large number corresponding to a density of $10^{11}$ to $10^{12}$ $cm^{-2}$. At higher magnification (Fig. 2) the untreated sample shows the contrast of atomic columns corresponding to an f.c.c.-lattice for both beam directions along [001] and [011].

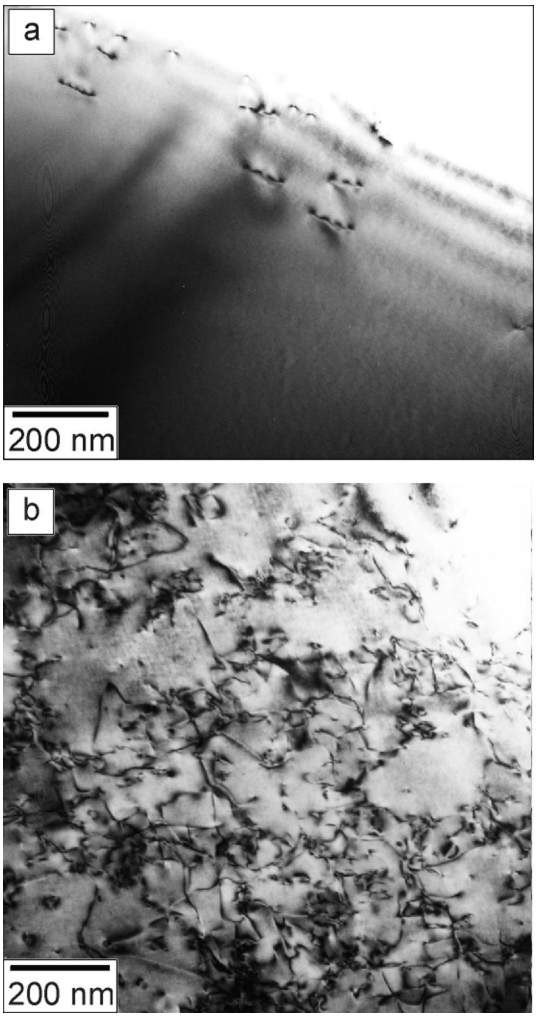


Fig. 1. TEM micrograph of an untreated (a) and a HHT (b) $Pd_{80}Pt_{20}$ sample revealing the increase in dislocation density.

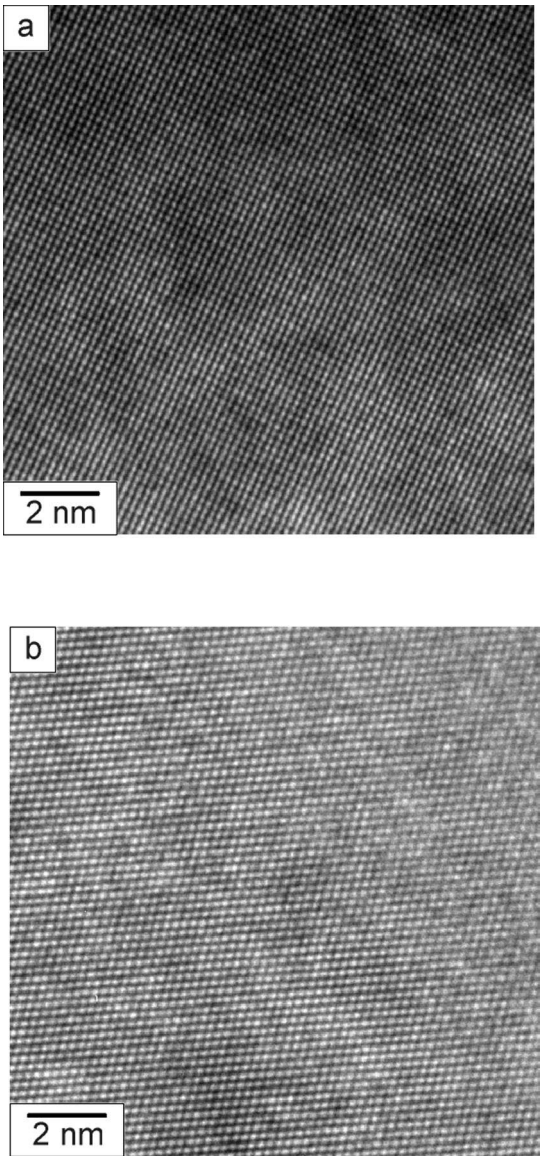


Fig. 2. HREM image of an untreated $Pd_{80}Pt_{20}$ sample. (a) Parallel to the [001] zone axis; (b) parallel to the [011] zone axis.

After HHT and projection along a [011] zone axis (Fig. 3), elongated plates can be observed with an angle of 109° in the plane perpendicular to the [011] zone axis. The plates have a diameter of ~8 nm and a thickness of about two (111) lattice planes, i.e. 0.45 nm. Estimating the density of plates leads to a volume fraction of $0.2(\pm 0.05)$. These observations are consistent with coherent precipitates formed as plates with their large interface parallel to {111} lattice planes. Two of these planes are parallel to the zone axis and intersect the (011) plane yielding the observed angle of 109°. The remaining two {111} planes are inclined so much with respect to the beam that they do not give enough contrast to be visible.

In Fig. 4 the same sample is examined in the close neighborhood of the [001] zone axis. Again elongated plates are detected with an angle of 90° in the plane

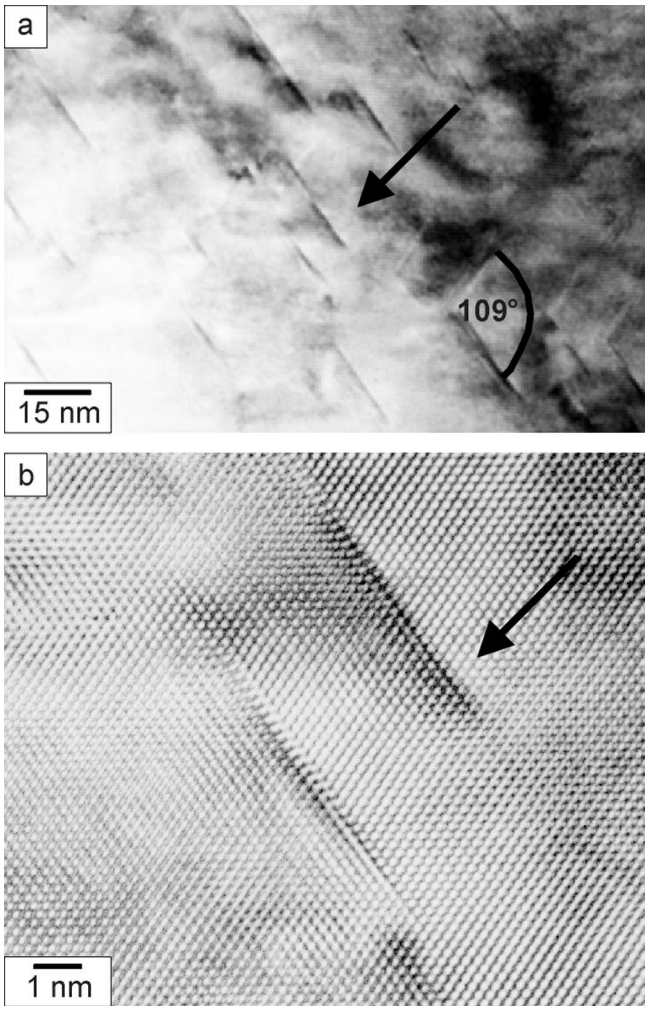


Fig. 3. HREM image for the HHT $Pd_{80}Pt_{20}$ sample with an illumination parallel to the [011] zone axis and for two different magnifications. Plate like features form an angle of 109°.

perpendicular to the [001] zone axis. The contrast is especially pronounced for dark field imaging using one of the (200) diffracted beams. The diffraction pattern reveals streaks inclined 45° to one of the ⟨002⟩ directions in reciprocal space corresponding to a reduced thickness along a ⟨111⟩ direction in real space. The plates are shown in Fig. 5 at a higher magnification. Again these observations are in agreement with thin plates lying parallel to the {111} planes of the matrix. For the [001] zone axis all four {111} planes intersect the (001) plane with the same angle (cf. Fig. 6) and, therefore, can be observed. All lines of intersection form an angle of 90° in agreement with experiment. Because the plates are not parallel to the electron beam (along [001], cf. Fig. 6) their projection increases in thickness by a factor of ~2 under these imaging conditions when compared with Fig. 3 for the [011] zone axis.

About ten diffusion coefficients were measured for each of the four samples at 298 K at different H-concentrations ranging from $10^{-4}$ to $10^{-2}$ (H-atoms)/(Me-atoms), i.e. in a dilute region where the diffusion coefficients do not

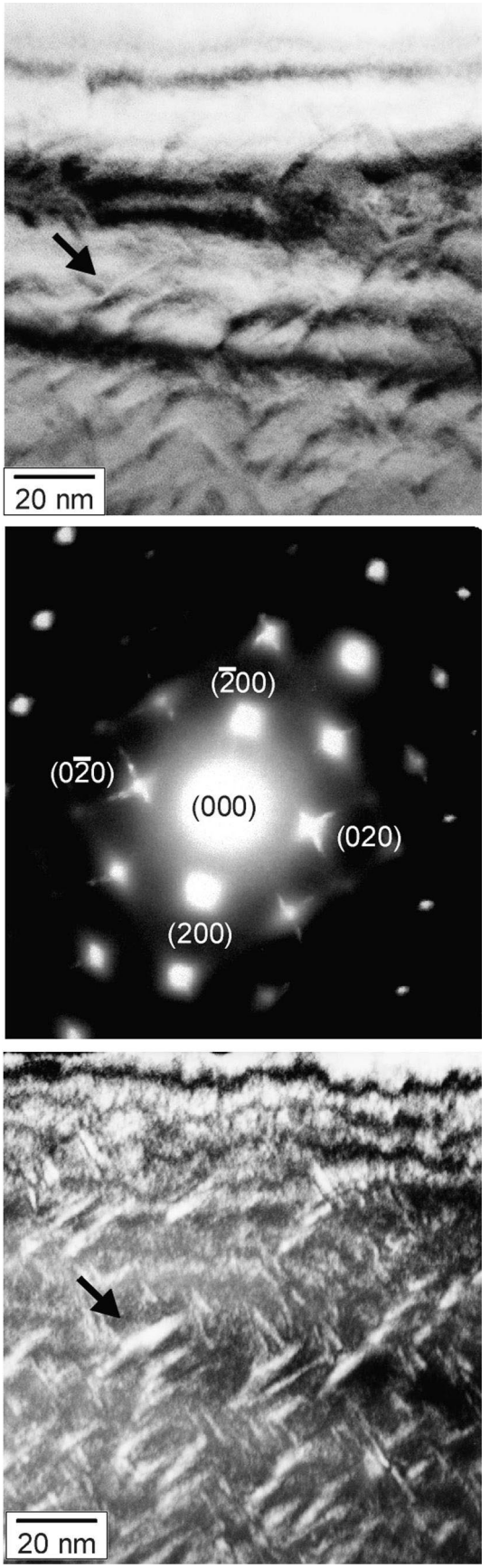


Fig. 4. Bright field (a) and dark field (c) image of a HHT $Pd_{80}Pt_{20}$ sample with an illumination parallel to the [001] zone axis. The corresponding diffraction pattern is shown in (b) revealing streaks.

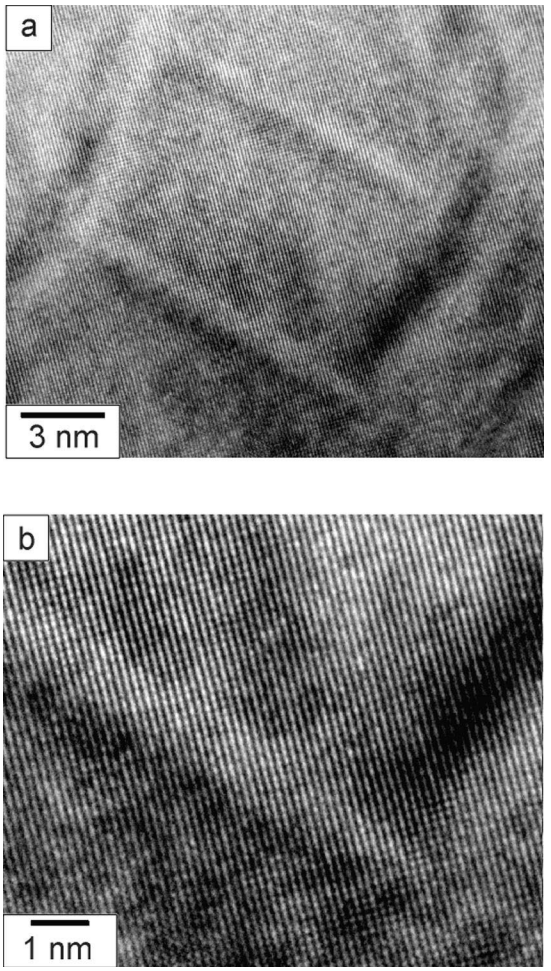


Fig. 5. HREM of an area shown in Fig. 4. The plate like features form an angle of 90°.

depend on H-concentration. The average values of the diffusion coefficients are given in Table 1.

Inspection of Table 1 clearly shows that the diffusion coefficients increase after HHT. In all cases the values are in-between those for pure Pd and pure Pt.

## 3. Discussion

By assuming reasonable interaction potentials between the constituents, Pd and Pt, the contrast observed in Fig. 3 was simulated. The supercell used and shown in Fig. 7 was ~15×5.5×10 nm in size and contained ~70,000 atoms. In the middle of the cell the composition of two (111) planes forming a disc with a diameter of 11 nm was changed from Pd- to Pt-rich compared to the surrounding matrix. Thus plate like precipitates are generated and relaxation was allowed inside the supercell with free surfaces normal to [011], whereas periodic boundary conditions were applied in the remaining two directions. Image simulations with 1024×1024 plane electron waves are shown in Fig. 8, which reveal that the dark appearance of the plates in Fig. 3 is obtained with Pt-rich precipitates. The concentrations used for the two phases were chosen according to the values estimated from the pc-isotherms (see below). Simulations with 2.5 and three layers of the second phase yielded dark regions which were thicker than the experimentally observed features. In addition the contrast of dislocation loops of the same lateral extension as the precipitates was simulated for the loops being either formed by vacancy or self-interstitial condensation. In both cases the contrast was totally different when compared with the observations in the HHT samples. Details of the whole procedure are described elsewhere [5].

The volume fraction of the precipitates of $0.2\pm0.05$ obtained from TEM is smaller than the value of 0.4 estimated from the isotherm. However, one has to take into account that the first one relates to substitutional sites and the latter to interstitial sites. For a thickness of the precipitates corresponding to two {111}-lattice planes of the metal atoms, three {111}-lattice planes of the lattice of octahedral sites (f.c.c. as well) will have a Pt-rich nearest neighborhood being unfavorable for H-occupancy. Thus a volume fraction $3\times(0.2\pm0.05)/2\approx0.3\pm0.08$ affects the isotherms as defined in Ref. [2].

For a random distribution of circular plates of a radius of 4 nm, a thickness of 0.45 nm and a volume fraction of 0.2, their centers have an average distance of 4.8 nm which is close to the value of 3.7 nm observed by SANS [2]. An exact comparison of the two results is difficult because the SANS correlation peak stems mostly from neighboring plates with a well defined orientation relationship.

Finally the same conclusion can be drawn as in Ref. [2] that HHT leads to phase separation with Pt-rich regions surrounded by a continuous Pd-rich matrix; however, compared to the indirect reasoning in Ref. [2] it is proven directly in this study. The changes of the H-diffusion coefficients provide additional support for this morphology. The increase of diffusion after HHT shows that it takes

Table 1
H-diffusion coefficients averaged over about ten different H-concentrations in $Pd_{85}Pt_{15}$ and $Pd_{80}Pt_{20}$ at 298 K before and after HHT

| Sample | $Pd_{85}Pt_{15}$ untreated | $Pd_{85}Pt_{15}$ HHT | $Pd_{80}Pt_{20}$ untreated | $Pd_{80}Pt_{20}$ HHT | Pd | Pt |
|---|---|---|---|---|---|---|
| $D$ ($10^{-7}$ cm$^2$ s$^{-1}$) | $1.34\pm0.04$ | $2.06\pm0.06$ | $1.28\pm016$ | $1.51\pm0.46$ | 3.7 | 1.0 |

Values for pure Pd and Pt are shown [4] for comparison.

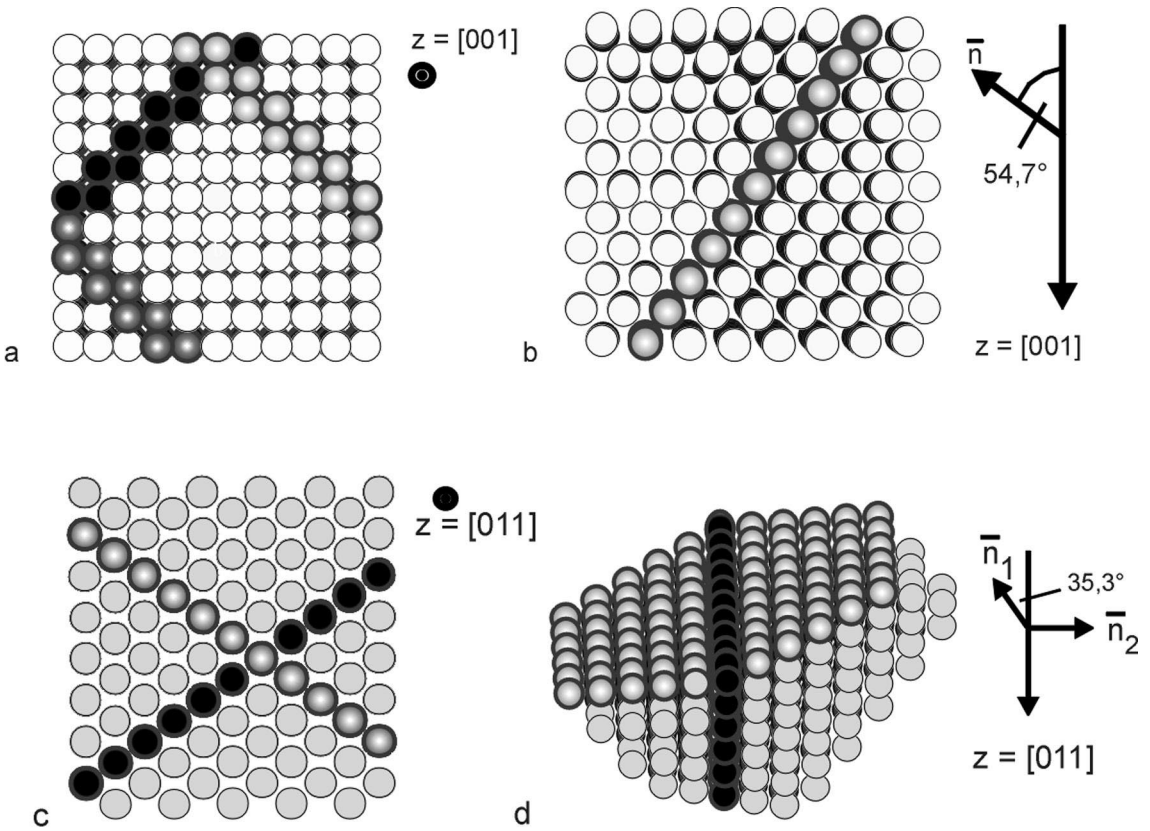


Fig. 6. Visualization of the arrangement of {111} lattice planes for the two zone axes z=[001] and z=[011] and for top view (a and c) and side view (b and d).

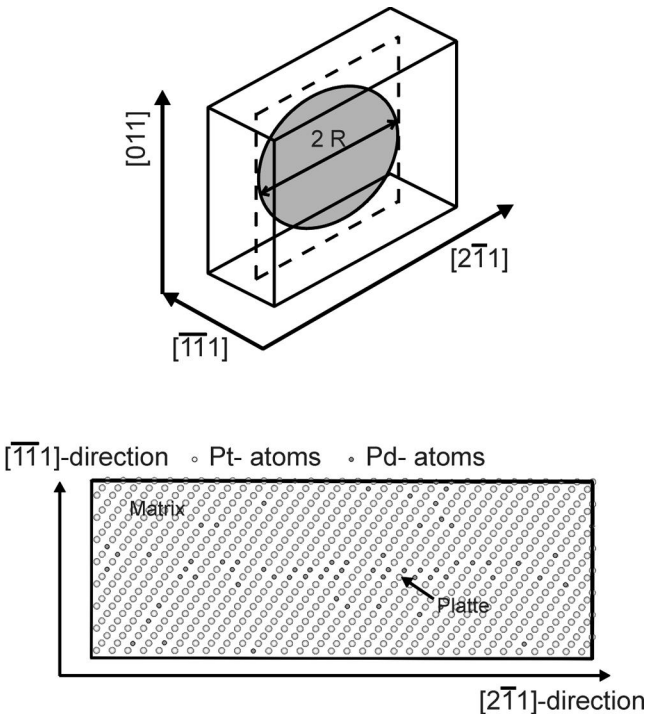


Fig. 7. Supercell employed and the arrangement of the disc shaped precipitate.

place in a Pd-rich phase which is continuous and where the Pt-rich inclusions act as obstacles which have to be circumvented. Although the latter effect counteracts the faster diffusion in Pd-richer alloys, it is reasonable to assume that it will not play a major role, because an excluded volume does not affect diffusivity very much [6]. For Pd-rich inclusions in a Pt-matrix, the lower site energies in the first phase would give rise to trapping and, therefore, a decrease of H-diffusivity would be expected in contradiction to the experimental findings.

Taking all experimental observations into consideration, the microscopic scenario of HHT may be as follows. After reaching a certain H-activity in Pd–Pt alloys, hydrides form as nuclei and grow. As in pure metals [7] the associated large volume increase leads to the formation of interstitial type dislocation loops. In this way extra matter is removed from the forming hydride to accommodate the local volume misfit. If Pt- and Pd-atoms have a certain mobility which may be enhanced in the presence of the dislocations (defines the onset temperature of HHT), Pt-atoms are preferentially expelled from the forming hydride because Pd-rich hydrides have a lower free energy [8]. The interstitial loop may be the precursor of the observed Pt-rich precipitates with the corresponding dislocation

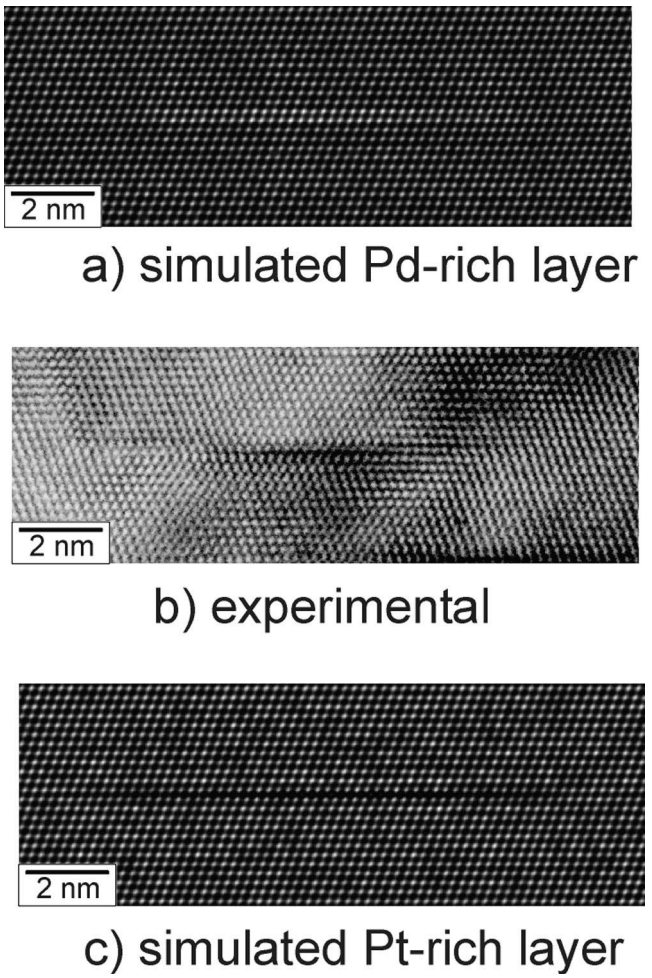


Fig. 8. Simulated contrast for a Pd-rich (a) and a Pt-rich (c) layer in comparison with the experimentally observed contrast (b).

being annihilated during hydrogen desorption at room temperature, where the mobility of Pd and Pt is too low to annihilate the non-homogeneous metal atom distribution. It may also be that the Pt-atoms expelled from the forming hydrides arrange themselves in the form of discs to reduce the overall strain energy.

## Acknowledgements

The authors are thankful for technical support from Ch. Borchers and M. Seibt during the TEM studies and for measurement of the diffusion coefficients by Ph. Kesten. Financial support by the Deutsche Forschungsgemeinschaft (SFB 345) is gratefully acknowledged.

## References

[1] H. Noh, J.D. Clewley, T.B. Flanagan, Scripta Mater. 34 (1996) 665.
[2] T.B. Flanagan, J.D. Clewley, H. Noh, J. Barker, J. Sakamoto, Acta Mater. 46 (1998) 2173.
[3] R. Kirchheim, Progr. Mater. Sci. 32 (1988) 262.
[4] E. Fromm, E. Gebhardt, Gase und Kohlenstoff in Metallen, Springer, Berlin, 1976, p. 638, p. 648.
[5] R. Lüke, PhD Thesis, University of Göttingen, 1999.
[6] E. Albert, E. Fromm, R. Kirchheim, Metall. Trans. 14A (1983) 2117.
[7] H.C. Jamieson, G.C. Weatherly, F.D. Manchester, J. Less-Common Met. 50 (1976) 85.
[8] C.-N. Park, T.B. Flanagan, Scripta Mater. 37 (1997) 1709.